Physics Faculty Publications and Presentations   Department of Physics

5-7-2015

Heterojunction Metal-Oxide-Metal Au-Fe₃O₄-Au Single Nanowire Device for Spintronics

K. M. Reddy
Boise State University

Nitin P. Padture
Brown University

Alex Punnoose
Boise State University

Charles Hanna
Boise State University

CrossMark
click for updates

Heterojunction metal-oxide-metal Au-Fe$_3$O$_4$-Au single nanowire device for spintronics

K. M. Reddy,[1,a)] Nitin P. Padture,[2] Alex Punnoose,[1] and Charles Hanna[1]

[1]*Department of Physics, Boise State University, Boise, Idaho 83725, USA*
[2]*School of Engineering, Brown University, Providence, Rhode Island 02912, USA*

In this report, we present the synthesis of heterojunction magnetite nanowires in alumina template and describe magnetic and electrical properties from a single nanowire device for spintronics applications. Heterojunction Au-Fe-Au nanowire arrays were electrodeposited in porous aluminum oxide templates, and an extensive and controlled heat treatment process converted Fe segment to nanocrystalline cubic magnetite phase with well-defined Au-Fe$_3$O$_4$ interfaces as confirmed by the transmission electron microscopy. Magnetic measurements revealed Verwey transition shoulder around 120 K and a room temperature coercive field of 90 Oe. Current–voltage (I-V) characteristics of a single Au-Fe$_3$O$_4$-Au nanowire have exhibited Ohmic behavior. Anomalous positive magnetoresistance of about 0.5% is observed on a single nanowire, which is attributed to the high spin polarization in nanowire device with pure Fe$_3$O$_4$ phase and nanocontact barrier. This work demonstrates the ability to preserve the pristine Fe$_3$O$_4$ and well defined electrode contact metal (Au)–magnetite interface, which helps in attaining high spin polarized current. © 2015 AIP Publishing LLC.
[http://dx.doi.org/10.1063/1.4913891]

Nanoscale building blocks present an exciting "bottom-up" paradigm for incorporating active component into electronic circuits for numerous multifunctional nanoelectronic devices.[1,2] 1-D inorganic oxide nanoscale components in the form of nanowires, nanoribbons, nanotubes, and nanorods are extensively studied owing to their unusual size dependent properties for delivering the device functionality.[1–5] Multifunctional magnetic nanowires (metal or oxide) have received much attention due to their potential application in perpendicular data recording, spintronics devices, scanning tips in magnetic force microscope, and in other biological applications.[6–11] Among them, magnetite (Fe$_3$O$_4$) have garnered much consideration for magnetoresistance[12,13] and spin filter device applications.[14]

Magnetite has been the subject of extensive research efforts because of high spin polarization and above room temperature Curie temperature, which finds applications in magneto-electronics. A room temperature ferromagnet with 858 K curie temperature and 100% spin polarization at the Fermi level with majority spin electrons exhibiting insulating or semiconducting behavior while the minority spins showing the metallic behavior has rendered the Fe$_3$O$_4$ to be obvious choice for magneto-electronics.[15] Spin polarization or magneto-electronic measurements on Fe$_3$O$_4$ were probed through electrical contacts to the oxide via evaporated metal electrodes,[12] or via spin-polarized electron spectroscopy,[16] or electron holography.[17] Magnitude of the spin polarized current was found to depend on material microstructure, grain size, grain boundary, defects, strain effects, and surface/interface reconstruction.[18] Much of the research in this area is on oxides

in the form of either bulk, compact powders,[15] epitaxial or continuous thin films,[19] epitaxial core-shell nanowires,[12] and more recently in the form of all oxide nanowires.[14] Magnetoresistance in these structures is credited to tunneling of spin-polarized electrons across the antiferromagnetically coupled antiphase/grain boundaries or interparticle contacts.[12,15,20] The above device structures involve complex transport channels and expose pristine Fe$_3$O$_4$ segment to suffer from device fabrication procedures resulting in defects, surface contamination and/or oxidation in addition to electrode interface/barrier effects. Low dimensionality and shape anisotropy have affected unique electron-transport behavior in 1D magnetic nanostructures.[12,21,22] Unsurpassed magnetoresistance studies require a novel architectural device with Fe$_3$O$_4$ 1D nanostructures where magnetic domains, nanocrystalline or single crystalline grains aligned in series. Additionally, Fe$_3$O$_4$ is thermodynamically unstable with respect to Fe$_2$O$_3$ in the presence of oxygen, known to suffer from surface reconstruction that hinders the path for spin-polarized current, predominantly at the electrode interface.

In this context, metal-oxide-metal (MOM) heterojunction nanowires,[23,24] where Fe$_3$O$_4$ nanoscale segment is sandwiched between two similar or dissimilar noble-metal nanowires are more representative of prototypical single nanowire device with high quality electrical contacts, which likely have some distinct advantage over all-oxide Fe$_3$O$_4$ nanowires. This type of geometry provides high quality, end-on electrical contact to the oxide directly circumventing all the device fabrication process. Unlike thin films, the MOM nanowires allow direct measurements of basic properties of nanoscale Fe$_3$O$_4$ segment without substrate-induced strain. Thus, the MOM nanowire architecture may prove to be very valuable in performing the fundamental studies related to

a)Author to whom correspondence should be addressed. Electronic mail: mrkongara@boisestate.edu.

magnetoresistance with direct relevance to the development of future spintronics devices. Here, we report the evidence of magnetoresistance in individual MOM nanowires with Au-Fe_3O_4-Au configuration.

Fe_3O_4 in the form of polycrystalline or epitaxial thinfilms and nanowires were successfully electrodeposited previously. However, it is difficult to synthesize Au-Fe_3O_4-Au nanostructures in the porous template because of diminished conductivity from Fe_3O_4 segment, which could be used as a back electrode for depositing top Au layer. Alternatively, Au-Fe-Au nanowires were synthesized using a template-based electrochemical method described by Tresback *et al.*[24] Briefly, sequential segments of Au(~2 μm), Fe (500 nm), and Au (~2 μm) were electrodeposited at a constant current 0.5 mA into the pores of anodic aluminum oxide (AAO) templates (with mean pore diameter ~250 nm) (Anapore®, Whatman, Inc., Florham Park, NJ). The all-metal Au-Fe-Au segments were released from template by dissolving anodic alumina template in aqueous NaOH solution and washed thoroughly. The nanowire segments were then concentrated and dispersed onto 1 μm SiO_2/Si substrates for further analysis. Then nanowires were subjected to extensive heat treatment analysis for determining the appropriate conditions for Fe to Fe_3O_4 phase transformation. Au-Fe_3O_4-Au nanowires were then characterized using a scanning electron microscope (SEM) (Sirion, FEI, Hillsboro, OR) and a transmission electron microscope (TEM) (Tecnai F20, FEI, Hillboro, OR) for microstructure and phase identification. A superconducting quantum interference device (SQUID) magnetometer was used to probe the magnetic properties of Au-Fe_3O_4-Au nanowires.

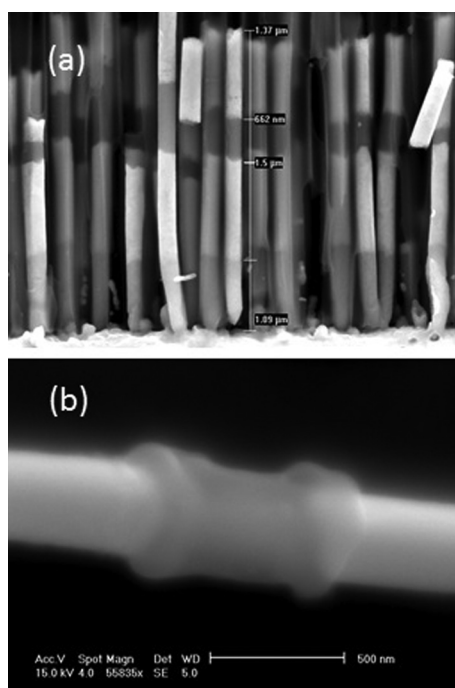Figure 1(a) (top) shows scanning electron microscopy image of Au-Fe-Au nanowires in the porous alumina template (cross section) synthesized in this study. The nanowire diameter is ~250 nm and the Fe segment is ~500 nm long. After dissolving the template, nanowires were dispersed onto SiO_2 wafer. Unlike template-free methods, the template-assisted synthesis used here can produce a very large number of nearly identical, high-definition heterojunction MOM nanowires that do not require sorting.[23,24] After extensive heat treatment analysis, it is found that the nanowires annealed at 225 °C for 20 h in a controlled atmosphere, 5% H_2 (balance N_2) with a 20 sccm flow successfully yielded the Au-Fe_3O_4-Au segment. With the above controlled oxidation conditions, Fe segment directly transformed into Fe_3O_4.[25,26] Other heat treatment conditions produced mostly Fe_2O_3 phase. SEM image of individual Au-Fe_3O_4-Au nanowire is shown in Figure 1(b) (bottom). Noticeably, the oxide segment that is sandwiched between two Au nanowire segments has swelled, because of the larger lattice volume of Fe_3O_4 compared to Fe. Figure 2(a) (bottom) displays TEM from an isolated nanowire after controlled oxidation process with clearly defined Au nanorods on each end of Fe_3O_4 segment. TEM studies indicated that Fe_3O_4 is polycrystalline with less than 10 nm grain size. Selected area electron diffraction, shown in Figure 2(b) (top left), confirms the oxide part of the nanowire a polycrystalline cubic magnetite (Fe_3O_4). The most intense Fe_3O_4 peak observed correspond to (311) plane. Smaller intensity peaks corresponding to (111), (220), (222), (400), (422), (511), and (440) were also identified. Energy dispersive X-ray analysis presented in Figure 2(c) (top right) also confirmed the presence of Fe and O in oxide segment. Further, no Au was observed in, or on the surface of Fe_3O_4 segments, precluding any possibility of electrical shorting.

Magnetic measurements on the heat-treated nanowires dispersed onto a SiO_2 wafer were performed using a SQUID magnetometer. Room temperature magnetic hysteresis was collected on a collection of Au-Fe_3O_4-Au nanowires. A saturation magnetization is attained for the nanowires at ~2000 Oe applied field and 95 Oe coercivity was observed, as shown in Figure 3, indicating room temperature ferromagnetism. A clear saturation magnetization is observed but the magnitude could not be estimated because of the nature of small Fe_3O_4 segment. Magnetic susceptibility measurements were carried out on Au-Fe_3O_4-Au nanowires to study possible phase transitions associated with temperature (5–300 K) and/or magnetic field dependence. Figure 4 shows zero-field cooled (ZFC) and field cooled (FC) magnetization for Au-
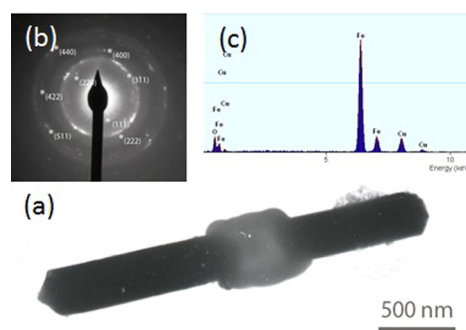

FIG. 1. (a) SEM cross sectional image of Au-Fe-Au nanowires in AAO template and (b) SEM image of a single Au-Fe_3O_4-Au nanowire after heat treatment.

FIG. 2. (a) TEM image of a single Au-Fe_3O_4-Au nanowire after heat treatment with defined electrode interfaces. (b) Selected area electron diffraction pattern of heterojunction nanowire presenting magnetite phase. (c) Energy dispersive X-ray analysis confirming Fe and O presence.
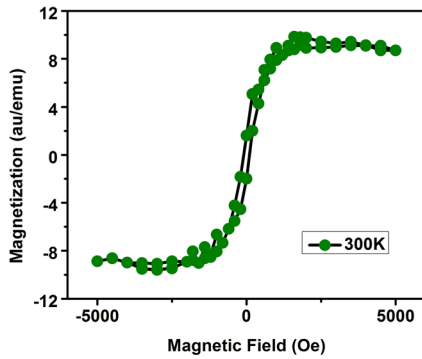
FIG. 3. Room temperature hysteresis plot on an Au-Fe$_3$O$_4$-Au nanowires dispersed on a substrate.

FIG. 5. Current (I)-voltage (V) characteristics of a single Au-Fe$_3$O$_4$-Au nanowire device, (inset) optical image of a device.

Fe$_3$O$_4$-Au nanowires with a 500 Oe applied magnetic field. With increasing temperature the magnetization increases with a shoulder around 120 K for ZFC measurements, which coincides with the Verwey transition in Fe$_3$O$_4$.[15] Considering the Fe$_3$O$_4$ content on the substrate, the small but clear shoulder is attributed to the Verwey transition. Owing to the room temperature coercivity observed in this study, superparamagnetism is discredited within these nanowires. Due to nanosize regime of the Fe$_3$O$_4$, Verwey transition effect is diminished. The broadening of Verwey transition can be explained on the basis of size effects[27] and/or precise Fe$_3$O$_4$ stoichiometry.[28] At the Verwey transition, Fe$_3$O$_4$ undergoes a charge ordering and structural ordering in the crystal lattice with crystallographic phase changing from cubic inverse spinel to monoclinic, and electrical properties undergo a metal-insulator transition as the temperature drops below 120 K.

Several individual MOM nanowire devices were fabricated using the procedure described elsewhere.[23] The inset of Figure 5 shows the low magnification optical micrographs of a typical single MOM nanowire device thus fabricated with the functional Fe$_3$O$_4$ segment with ∼250 nm thickness and 500 nm in length. Note that the Fe$_3$O$_4$ segment of the MOM nanowire is not attached to the substrate mechanically, and the metal nanowires provide no mechanical constraint, hence no substrate-induced strain is expected in the Fe$_3$O$_4$ segment.[23]

Figure 5 shows the typical current–voltage response at various temperatures from an individual Au-Fe$_3$O$_4$-Au nanowire device showing Ohmic behavior. This data indicate a good interface contact between the Au electrodes and
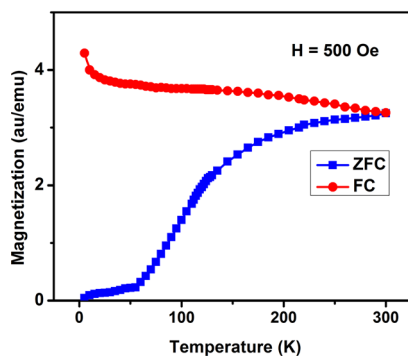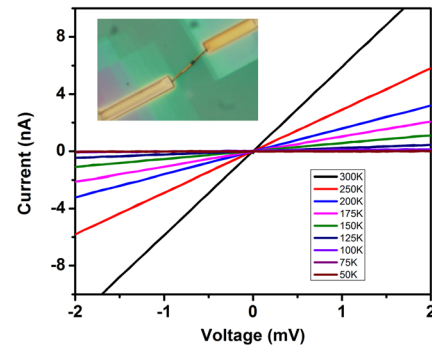
functional Fe$_3$O$_4$ segment. Figure 6 shows the resistance variation with temperature, derived from I-V plot at a constant voltage bias. Room temperature electrical resistivity of individual heterojunction nanowire is found to be around 6.6 × 10^{-3} Ω cm, which is comparable to the bulk but higher than epitaxial thin films of Fe$_3$O$_4$.[29,30] The higher resistance in Au-Fe$_3$O$_4$-Au nanowire could point towards the electrode-interface connectivity or grain boundary resistance with the smaller grains, as in the case of bulk. The inset of Figure 6 shows Arrhenius plot (ln (R) against 1000/T) that highlights the charge transport mechanism due to thermal activated electron hopping. Activation energy found to be around 0.05 eV above 125 K, which is in good agreement with the nanowire/nanotube morphology of Fe$_3$O$_4$ system.[12,31] Resistance below 120 K seems to be very high due to freezing up of charge carriers, which is rendered to Verwey transition in Fe$_3$O$_4$ system.

Figure 7 shows magnetoresistance response from an individual Au-Fe$_3$O$_4$-Au heterojunction nanowire device at room temperature. Magnetic field is swept parallel to the nanowire from 0 to 5 T keeping a constant voltage bias. Magnetoresistance defined in this article is calculated as MR = [R(H) − R(0)]/R(0), where R(0) and R(H) are resistance at zero field and at an applied field, H, respectively. Magnetoresistance observed on the nanowire was very small and was too noisy because of the small signal resulting from 250 nm wide × 500 nm long Fe$_3$O$_4$ segment. An anomalous positive magnetoresistance, less than 1%, is observed with the nanowire at room temperature under a 5 T magnetic field.

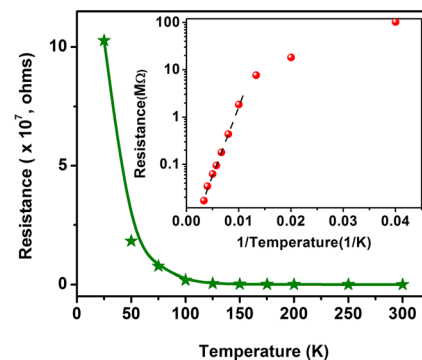FIG. 4. Zero-field cooled and field cooled magnetization scans with temperature at an 500 Oe applied field.

FIG. 6. Resistance variation with temperature of a single Au-Fe$_3$O$_4$-Au nanowire device, (inset) corresponding Arrhenius plot showing a linear increase in activation energy above 120 K.
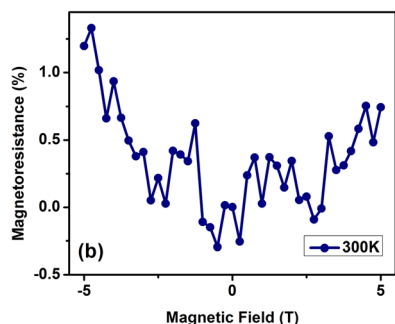
FIG. 7. Positive magnetoresistance (<1%) from an Au-Fe_3O_4-Au nanowire at 300 K.

Positive magnetoresistance observed in this nanowire is contrary to the vast majority of studies among epitaxial thin films, single crystal and bulk Fe_3O_4.[15,21,22] Still, it is not uncommon to see positive magnetoresistance in Fe_3O_4 nanowire,[14] thinfilm and bulk systems.[32–34] However, positive and negative magnetoresistance effect is observed in Fe_3O_4 heterostructures.[35] In bulk and thin film Fe_3O_4 systems, magnetoresistance is attributed to the filed-induced alignment of grains or antiphase domains.[20,36] Exclusive positive magnetoresistance is attributed to the nanocontact barrier,[37] and high degree of spin polarization in Fe_3O_4 in addition to a pristine electrode–Fe_3O_4 interface, as suggested by Liao *et al.*[14] Functional Fe_3O_4 segment is only 500 nm long and 250 nm in diameter without any substrate induced-strain. Cross-sectional Au electrode interface is only 250 nm on either sides of Fe_3O_4 greatly reducing the resistances associated with multiple interfaces and tunneling channels. Nevertheless, magnetoresistance in Fe_3O_4 systems has been very contentious.

In summary, we report on the template-based synthesis of high-definition MOM heterojunction Au-Fe_3O_4-Au nanowire system. The dimensions of these nanowire devices can be easily manipulated for incorporating individual Au-Fe_3O_4-Au nanowire in high-quality devices, further excluding substrate-induced strain effects. This study demonstrates the ability to understand the fundamental device behavior of low dimensional materials. Our work validates the evidence of magnetoresistance in Au-Fe_3O_4-Au nanowire suggesting that spin based device integration can be realized with well-defined functional segments.

[1]C. M. Lieber, "The incredible shrinking circuit—Researchers have built nanotransistors and nanowires. Now they just need to find a way to put them all together," Sci. Am. **285**(3), 58–64 (2001).

[2]Z. W. Pan *et al.*, "Nanobelts of semiconducting oxides," Science **291**(5510), 1947–1949 (2001).

[3]Y. N. Xia *et al.*, "One-dimensional nanostructures: Synthesis, characterization, and applications," Adv. Mater. **15**(5), 353–389 (2003).

[4]Z. L. Wang, "Nanobelts, nanowires, and nanodiskettes of semiconducting oxides—From materials to nanodevices," Adv. Mater. **15**(5), 432–436 (2003).

[5]C. M. Lieber *et al.*, "Functional nanowires," MRS Bull. **32**(2), 99–108 (2007).

[6]M. Tanase *et al.*, "Magnetotransport properties of bent ferromagnetic nanowires," J. Appl. Phys. **93**(10), 7616–7618 (2003).

[7]D. H. Reich *et al.*, "Biological applications of multifunctional magnetic nanowires (invited)," J. Appl. Phys. **93**(10), 7275–7280 (2003).

[8]G. Reiss *et al.*, "Magnetic nanoparticles—Applications beyond data storage," Nat. Mater. **4**(10), 725–726 (2005).

[9]Y. L. Chueh *et al.*, "Systematic study of the growth of aligned arrays of alpha-Fe_2O_3 and Fe_3O_4 nanowires by a vapor-solid process," Adv. Funct. Mater. **16**(17), 2243–2251 (2006).

[10]A. Hultgren *et al.*, "Cell manipulation using magnetic nanowires," J. Appl. Phys. **93**(10), 7554–7556 (2003).

[11]R. Skomski, "Nanomagnetics," J. Phys.: Condens. Matter **15**(20), R841–R896 (2003).

[12]D. H. Zhang *et al.*, "Magnetite (Fe_3O_4) core-shell nanowires: Synthesis and magnetoresistance," Nano Lett. **4**(11), 2151–2155 (2004).

[13]C. Terrier *et al.*, "Fe_3O_4 nanowires synthesized by electroprecipitation in templates," J. Appl. Phys. **98**(8), 086102 (2005).

[14]Z. M. Liao *et al.*, "Spin-filter effect in magnetite nanowire," Nano Lett. **6**(6), 1087–1091 (2006).

[15]J. M. D. Coey *et al.*, "Magnetoresistance of magnetite," Appl. Phys. Lett. **72**(6), 734–736 (1998).

[16]J. G. Tobin *et al.*, "Spin resolved photoelectron spectroscopy of Fe_3O_4: The case against half-metallicity," J. Phys.: Condens. Matter **19**(31), 315218 (2007).

[17]M. T. Chang *et al.*, "Magnetic and electrical characterizations of half-metallic Fe_3O_4 nanowires," Adv. Mater. **19**(17), 2290 (2007).

[18]W. D. Wang, L. Malkinski, and J. K. Tang, "Enhanced spin-dependent tunneling magnetoresistance in magnetite films coated by polystyrene," J. Appl. Phys. **101**(9), 09J504 (2007).

[19]T. A. Sorenson *et al.*, "Epitaxial electrodeposition of Fe_3O_4 thin films on the low-index planes of gold," J. Am. Chem. Soc. **124**(25), 7604–7609 (2002).

[20]J. M. D. Coey *et al.*, "Half-metallic ferromagnetic oxides," MRS Bull. **28**(10), 720–724 (2003).

[21]Z. Q. Liu *et al.*, "Single crystalline magnetite nanotubes," J. Am. Chem. Soc. **127**(1), 6–7 (2005).

[22]K. Liu *et al.*, "Extrinsic magnetoresistance in magnetite nanoparticles," J. Appl. Phys. **93**(10), 7951–7953 (2003).

[23]E. D. Herderick *et al.*, "Bipolar resistive switching in individual Au-NiO-Au segmented nanowires," Appl. Phys. Lett. **95**(20), 203505 (2009).

[24]J. S. Tresback *et al.*, "Engineered metal-oxide-metal heterojunction nanowires," J. Mater. Res. **20**(10), 2613–2617 (2005).

[25]A. P. Grosvenor *et al.*, "Examination of the oxidation of iron by oxygen using X-ray photoelectron spectroscopy and QUASES (TM)," Surf. Sci. **565**(2–3), 151–162 (2004).

[26]X. N. Xu *et al.*, "Annealing study of Fe_2O_3 nanoparticles: Magnetic size effects and phase transformations," J. Appl. Phys. **91**(7), 4611–4616 (2002).

[27]G. F. Goya *et al.*, "Static and dynamic magnetic properties of spherical magnetite nanoparticles," J. Appl. Phys. **94**(5), 3520–3528 (2003).

[28]V. A. M. Brabers *et al.*, "Impurity effects upon the Verwey transition in magnetite," Phys. Rev. B **58**(21), 14163–14166 (1998).

[29]W. Kim *et al.*, "Fabrication and magnetoresistance of tunnel junctions using half-metallic Fe_3O_4," J. Appl. Phys. **93**(10), 8032–8034 (2003).

[30]W. Eerenstein *et al.*, "Origin of the increased resistivity in epitaxial Fe_3O_4 films," Phys. Rev. B **66**(20), 201101 (2002).

[31]L. Degiorgi *et al.*, "Small-polaron conductivity in magnetite," Phys. Rev. B **35**(17), 9259–9264 (1987).

[32]R. V. Chopdekar *et al.*, "Magnetics and magnetoresistance in epitaxial magnetite heterostructures," J. Electron. Mater. **33**(11), 1254–1258 (2004).

[33]J. H. Hsu *et al.*, "Anomalous positive magnetoresistance in Fe_3O_4-Ag composite films," J. Magn. Magn. Mater. **242**, 479–481 (2002).

[34]H. B. Gu *et al.*, "Magnetoresistive polyaniline-magnetite nanocomposites with negative dielectric properties," Polymer **53**(3), 801–809 (2012).

[35]L. Y. Zhang *et al.*, "Fabrication and magnetic properties of Fe_3O_4 nanowire arrays in different diameters," J. Magn. Magn. Mater. **321**(5), L15–L20 (2009).

[36]W. Eerenstein *et al.*, "Spin-polarized transport across sharp antiferromagnetic boundaries," Phys. Rev. Lett. **88**(24), 247204 (2002).

[37]A. Orozco *et al.*, "Oscillatory exchange coupling and giant positive magnetoresistance in TiN/Fe_3O_4 superlattices," Phys. Rev. Lett. **83**(8), 1680–1683 (1999).